

Interfacial Morphologies and Possible Mechanisms of Copper Wafer

Bonding

K. N. Chen, A. Fan and R. Reif

Microsystems Technology Laboratories

Massachusetts Institute of Technology, Cambridge, MA 02139, USA

E-mail: knchen@mit.edu

The microstructure morphologies of copper bonded wafers were examined by means of transmission electron microscopy (TEM) and atomic force microscope (AFM). Morphologies of non-distinct, zigzag and distinct interfaces in the bonded layer are observed. A strong relationship between the roughness of surfaces and the individual steps in bonding initiation was found. We propose three different mechanisms to explain the observed morphologies. In addition, the role of atomic diffusion and that of annealing effects during bonding is discussed.

1. Introduction

In microelectromechanical systems (MEMS), direct wafer bonding has become a mainstay for device applications such as SOI,[1] sensors and actuators.[2-3] Wafer bonding may also have a niche in integrated circuits by making possible the integration of devices fabricated with different technologies.[4] Based on this, IC design may become more flexible.[4-6] However, for wafer bonding to have an impact on the IC industry, the electrical, thermal, and mechanical properties of the bond has to be well characterized. Different CMOS-compatible materials suitable for wafer bonding are being investigated. For example, Si-Si bonding has attracted a great deal of attention. [1-4]

While significant process has been made to improve the process of silicon bonding, a complete understanding of the bonding mechanism is still under investigation. Several models [7-9] discuss wafer bonding as a function of the bonding wave velocity, bonding strength, and interfacial oxide thickness on pure silicon surface. Direct wafer bonding has been attributed to short-range intermolecular and interatomic attraction forces, such as Van der Waals forces. [10-11]

In comparison with Si-Si wafer bonding, research on thin-film metal-to-metal wafer bonding is still in its very early stage. The behavior of the metal-to-metal bond directly determines the circuit performance of the bonded structure, such as the electric resistance

of metal wire bonding area. This is especially true for Cu wafer bonding. Cu has low electrical resistivity, high electromigration resistance, and has already been integrated into the main stream interconnect technology. For these reasons, in the implementation of 3D integrated circuits, copper wafer bonding is a very attractive candidate.[12]

The interface morphologies and bonding strengths of several metal species have been examined.[11-14] For example, for sputter deposited Ti and Pt, Shimatsu et al. investigated the morphologies of the bonded layer.[13] Their results showed that successful bonding of these two metal species thin films occurred at room temperature over the entire area (12mm x 12mm). We studied the Cu interface morphologies and bond strengths under a variety of bonding conditions.[12] The qualitative bond strength of copper wafers was previously examined with the razor test. Silicon wafers, coated with 300 nm evaporated copper, were successfully bonded at 400°C for 30 min with a post-bonding anneal in N₂ for 30 min. For successful bonding, a post-bonding anneal is required. Different bonding conditions, such as bonding temperature, anneal temperature, anneal time, and copper layer thickness, were also examined.[11-12, 14]

Few reports discuss or propose mechanisms to explain the observed morphologies of the metal bonding. In particular, the relationship between interfacial morphologies and bonding parameters has received little attention. In this article, we investigate the

interfacial morphologies of bonded layers and propose mechanisms for copper wafer bonding.

2. Experimental

The experimental procedures are the same as in Reference 12. N-type (100) Si wafers with a 300nmCu/50nmTa film structure were used. The wafers were ready to be bonded in the Electronic Vision EV 450 Aligner and AB1-PV bonder after a dilute HCl dip to remove any Cu oxide on the surface. A 4000-mbar force was applied for 30 min at 400°C. After bonding, the wafers were annealed at 400°C in N₂ ambient for 30 min. The morphologies of the Cu-Cu bonded wafer interface were examined with a JEOL-200CX scanning transmission electron microscope (STEM) and JEOL-2010 transmission electron microscope. The surface morphology of cleaned Cu wafer before bonding was examined with an Autoprobe CP atomic force microscope (AFM). The crystallography of the Cu film was analyzed by X-ray diffraction (XRD) [Rigagu D/Max] with Cu K α radiation.

3. Results and Discussion

Cross sectional transmission electron (TEM) images of the Cu-Cu bonded layer taken from the center of the wafer are shown in Figs. 1 (a)-(f). These pictures show a “good” bond layer formed at the bonding condition. Random interfaces, grains, and

defects are observed, but no voids are found in the bonded layer. It is important that all of these morphologies can be observed in wafers bonded at the condition depicted in the experimental procedure. In addition, these morphologies are formed together randomly everywhere in the bonded layer. Figure 1(a) shows a low magnitude TEM image of Cu-Cu bonded layer.

Figure 1(b) shows there is no observable interface between two Cu layers after bonding. We also do not find any grain boundaries in this region. On the other hand, in Fig. 1(c), another kind of interface is observed: a zigzag interface with an average fluctuation depth (i.e., distance between the original interface and the grain boundary) of 30 nm. The dimension of the fluctuation depth could change drastically, up to 75 nm, as shown in Fig. 1(d). As shown in Fig. 1(c), a zigzag interface between two original Cu layers as well as grain structures in the films are observed. The intersection point of grain boundaries of the two original films at the interface is the turning point of the zigzag fluctuation. This morphology was also observed in Pt bonded layer in the paper of Shimatsu et al. [13] A smooth interface with a smaller fluctuation depth of 5 nm is observed in Fig. 1(e), and no grain boundaries are observed. We also found continuous twins, oriented 75 degrees with respect to the Si substrate, penetrate the bonded layer, as shown in Fig. 1(f). It should be noted that no voids are observed in the interface region in

these five images. We believe that these morphologies suggest that there is a strong relationship between the roughness of the original surfaces and the initial steps of bonding.

An atomic force microscope (AFM) was used to measure the wafer surface roughness. We investigated the surface roughness of the Cu wafer after HCl treatment but before bonding. Figure 2 shows that the surface roughness of this film was about 1.5 nm. It should be mentioned that this value is significantly smaller than the average fluctuation depth of the zigzag interface of 30 nm in the bonded layer (Fig. 1(c)). In addition, the roughness is not uniform everywhere on a microscopic scale.

Grain orientation and growth are also important during bonding. Figures 3(a) and (b) show XRD patterns of Cu film just deposited and bonded layer, respectively. In Fig. 3(a), Cu film shows (111) preferred grain orientation with very strong intensity and sharp curve. On the other hand, after bonding and anneal process, the bonded layer shows (220) preferred grain orientation. The intensity of original (111) preferred orientation becomes weak. The preferred orientation is completely different from that of before bonding. This suggests that recrystallization and grain growth have occurred during bonding and anneal process. In the research of Shimatsu et al., similar results were also observed in Ti and Pt samples. [13]

All wafer surfaces are rough on a microscopic scale, especially after a metal evaporation process. The asperities, which characterize the profile of the wafer surface, can have many spherical caps. During the wafer bonding, these asperities on the wafer surface would be in contact with those on the other wafer. Under “normal load” conditions (“normal load” is defined here as that perpendicular to the plane of the substrate surface), the contact region would deform and the atoms on the different wafers will interdiffuse.

It is well-known that, for good wafer bonding, the contact area and the bonding energy must be as large as possible. In addition, when the radii of the deforming elastic spheres decrease, larger contact forces are needed.[11] This suggests that wafers having small radius asperities are more difficult to bond. The smaller the contact area is, the smaller the force is needed to deform it.

When two Cu wafers with 1.5 nm surface roughness are in contact with each other under a normal load and a constant temperature higher than room temperature, the Cu atoms on the wafer surfaces are active and kinetically energized. We consider the following three possible mechanisms: (a) “peak-to-peak” contact of two surfaces with similar scale roughness, (b) “peak-to-valley” contact of two surfaces with similar scale roughness, and (c) contact of two surfaces under different scale roughness.

During “peak-to-peak” bonding, the contact area is small and the elastic spheres deform easily (see Fig. 4). Therefore, the distance between the two layers might be as small as an atom scale. Consequently, Cu atoms with higher kinetic energy could easily “jump” from one surface to another. During the bonding process, atoms on the surfaces increasingly interdiffuse into each other. At the same time, grain growth occurs. The interface eventually disappears and the two films become a homogeneous region. This mechanism may give rise to the morphology shown in Fig. 1(b).

It is important to discuss the interfacial behavior during post-bonding anneal. At a temperature higher than room temperature, recrystallization and grain growth may form during anneal, and the weak structures at the original interface area are strengthened. This may explain why annealing is a necessary step for a good wafer bond.[12] In, Fig. 1(f), twins oriented 75 degree with respect to the Si substrate were observed in the bonded layer. The twins are continuous and penetrate the bonded layer.

The bonding mechanism is different when the two surfaces are bonded under “peak-to-valley” conditions (see Fig. 5). The force acting on the contact area is smaller than the normal load due to the direction of normal load is not perpendicular to the contact area. The atoms on the surface are more flexible under high temperature and keep moving along the surface until the two surfaces match each other. During the anneal

treatment, grain growth occurs. Under this scenario, observed grains in the bonded layer would be similar to the zigzag interface in Fig. 1(c). In addition, we observe a large fluctuation in the interface from 30nm to 75 nm when there was a stronger grain growth during the bonding and anneal, as shown in Fig. 1(d).

Interfacial fluctuations would be even more visible if grain structure already exists before bonding. It is known that the diffusion rate of the atoms at the grain boundary is higher than that inside the grain. So, we also believe that grain boundary self-diffusion and interface diffusion play a greater role in bonding rather than bulk diffusion. If the surface roughness were similar to the fluctuation depth, the diffusion of surface atoms would not have been obvious. However, the surface roughness (about 1.5 nm) is sufficiently smaller than the fluctuation depth of the zigzag interface (30 nm). It suggests that the diffusion of surface atoms plays a dominant role during bonding.

When two contact regions have different scale of surface roughness (see Fig. 6), they do not match in size during bonding. According to previous discussion, small asperities are difficult to bond. However, under bonding pressure, asperities on the surfaces of both wafers would have to squeeze together, thereby decreasing the voids between the mismatched peaks and valleys. As a result, the small asperities would tend to move together to match the size of the valley at the other side then start to bond, as shown

in Fig. 6. This mechanism decreases the bonding energy. After bonding, some voids would remain at the interface, which would be removed during annealing. However, it is possible that an interface may still exist in the bonded layer because of inefficient anneal time and temperature, as shown in Fig. 1 (e). In addition, we notice that the fluctuation depth in Fig. 1(e) is much smaller than those in Figs. 1(c) and (d). On the other hand, it seems to match the original surface roughness of 1.5 nm. However, we do believe that the interface in this region would either disappear or become a zigzag shape if the anneal time had been longer. In the case of Fig 6., if the initial surface roughness is very high, there will be only a small contact area at the interface region during bonding. After bonding, permanent voids may be left at the interface. When the surface roughness is high enough, the wafers cannot bond at all.

4. Conclusion

In conclusion, various morphologies of non-distinct, zigzag, and distinct interfaces are observed in the Cu bonded layer. These morphologies suggest that there is a strong relationship between the roughness of surfaces and the initial steps of bonding. The change of preferred orientation indicates recrystallization and grain growth occur during bonding and anneal process. Possible mechanisms of copper layer bonding were presented. Three different types of mechanisms have been proposed to explain the

various interface morphologies of the bonded layer: “Peak-to-peak” contact of two surfaces with similar scale roughness, “peak-to-valley” contact of two surfaces with similar scale roughness, and contact of two surfaces under different scale roughness. These three mechanisms were used to explain the non-interface, zigzag interface and distinct interface, respectively, observed in the bonded layer. We propose that the wafer surface roughness is an important parameter during bonding. Furthermore, the surface diffusion of atoms and the anneal temperature play important roles in the Cu wafer bonding process.

Acknowledgements

This paper acknowledges support from the MARCO Focused Research Center on Interconnects which is funded at the Massachusetts Institute of Technology, through a subcontract from the Georgia Institute of Technology. The authors would like to thank Mr. Ioannis Kymissis (MIT) for AFM assistance.

REFERENCES

1. J. B. Lasky, *Appl. Phys. Lett.* **48**, 78 (1986).
2. P. W. Barth, "Silicon fusion bonding for fabrication of sensors, actuators and microstructures," *Sensors Actuators*, **A21-A23**, pp. 919-926 (1990).
3. M. A. Huff, A. D. Nikolich, and M. A. Schmidt, "A threshold pressure switch utilizing plastic deformation of silicon," in *Proc. 6th Int. Conf. Solid State Sensors Actuators*, San Francisco, Elsevier Science, June 24-27, 1991, pp. 177-180.
4. A. Fan and R. Reif, *Electrochemical Society Spring Meeting*, March 2001 (in press).
5. S. Bengtsson, *J. of Electro. Mat.* **21**, 841 (1992).
6. C. Y. Chang and S. M. Sze, *ULSI Technology*, p. 673, McGraw-Hill, New York (1996).
7. R. Stengl, T. Tan, U. Gosele, *Jpn. J. Appl. Phys.* **28**, 1735 (1989).
8. W. P. Maszara, *J. Electrochem. Soc.* **138**, 341 (1991).
9. L. Ling and F. Shimura, *J. Appl. Phys.* **71**, 1237 (1992).
10. Q.-Y. Tong and U. Gosele, *Mater. Chem. Phys.* **37**, 101 (1994).
11. C. Gui, M. Elwenspoek, N. Tas, and J. G. E. Gargeniers, *J. Appl. Phys.* **85**, 7448 (1999).

12. A. Fan, A. Rahman, and R. Reif, *Electrochemical and Solid-Sates Letters*, **2**,10

(1999).

13. T. Shimatsu, R. H. Mollema, D. Monsma, E. G. Keim and J. C. Lodder, *J. Vac. Sci.*

Technol. A **16(4)**, 2125 (1998).

14. K. N. Chen, A. Fan and R. Reif, *J. of Electro. Mat.* **30**, 331 (2001).

FIGURE CAPTIONS

Figures 1(a)-(f) XTEM images of the Cu-Cu bonded layer: (a) low magnitude image, (b) no observable interface, (c) zigzag interface, (d) drastically changing fluctuation depth, (e) the smooth interface with a smaller fluctuation depth, and (f) continuous twins.

Figure 2 AFM image of the surface roughness of Cu film before bonding.

Figure 3 XRD patterns for (a) Cu film just deposited, (b) Cu bonded layer.

Figure 4 Schematic diagram of “peak-to-peak” bonding mechanism.

Figure 5 Schematic diagram of “peak-to-valley” bonding mechanism.

Figure 6 Schematic diagram of “different scale roughness” bonding mechanism.

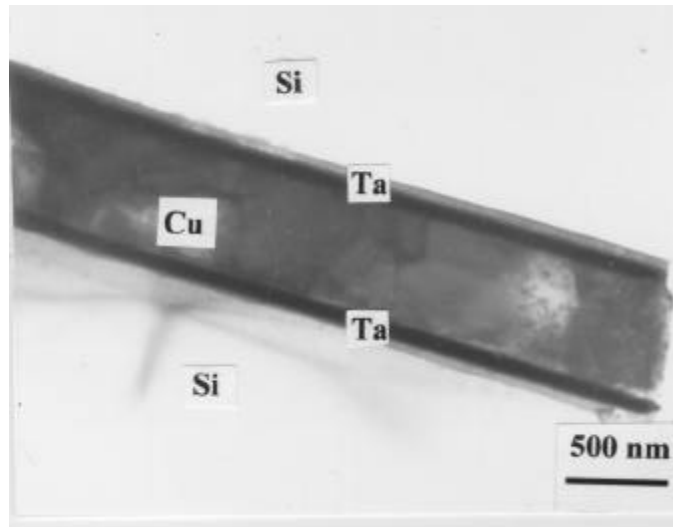


Figure 1(a)

Figures 1(a)-(f) XTEM images of the Cu-Cu bonded layer: (a) low magnitude image, (b) no observable interface, (c) zigzag interface, (d) drastically changing fluctuation depth, (e) the smooth interface with a smaller fluctuation depth, and (f) continuous twins.

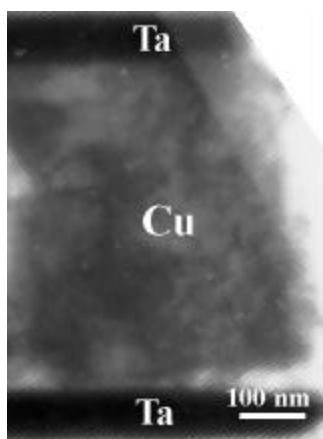


Figure 1(b)

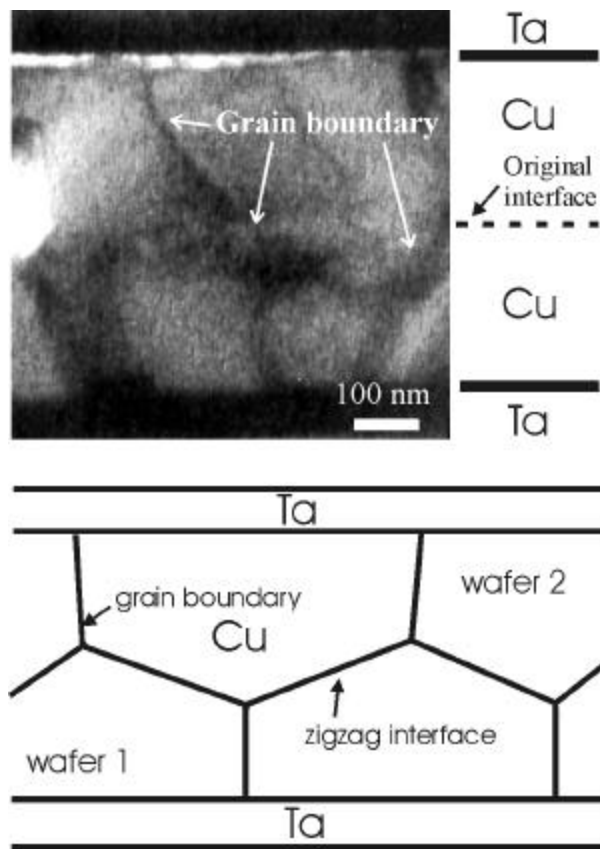


Figure 1(c)

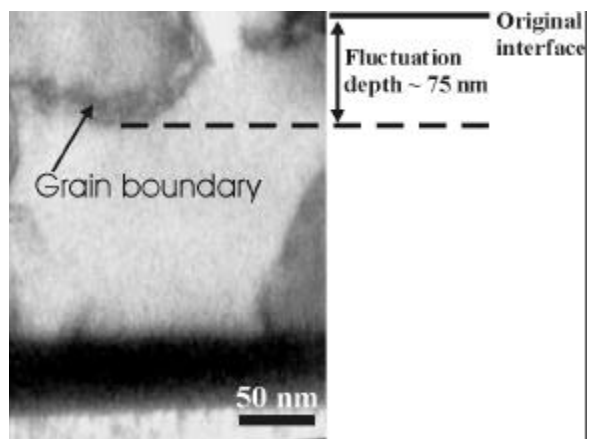


Figure 1(d)

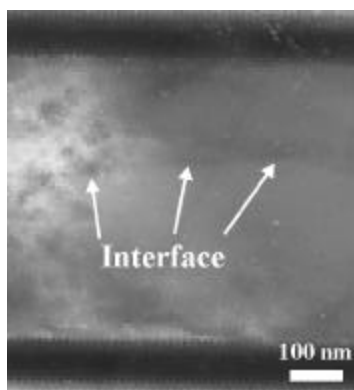


Figure 1(e)

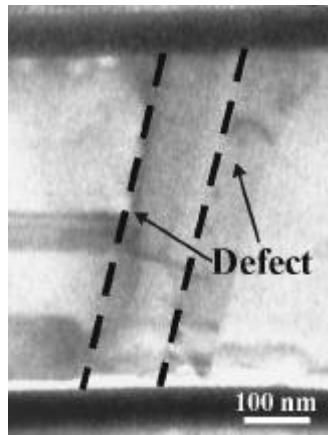
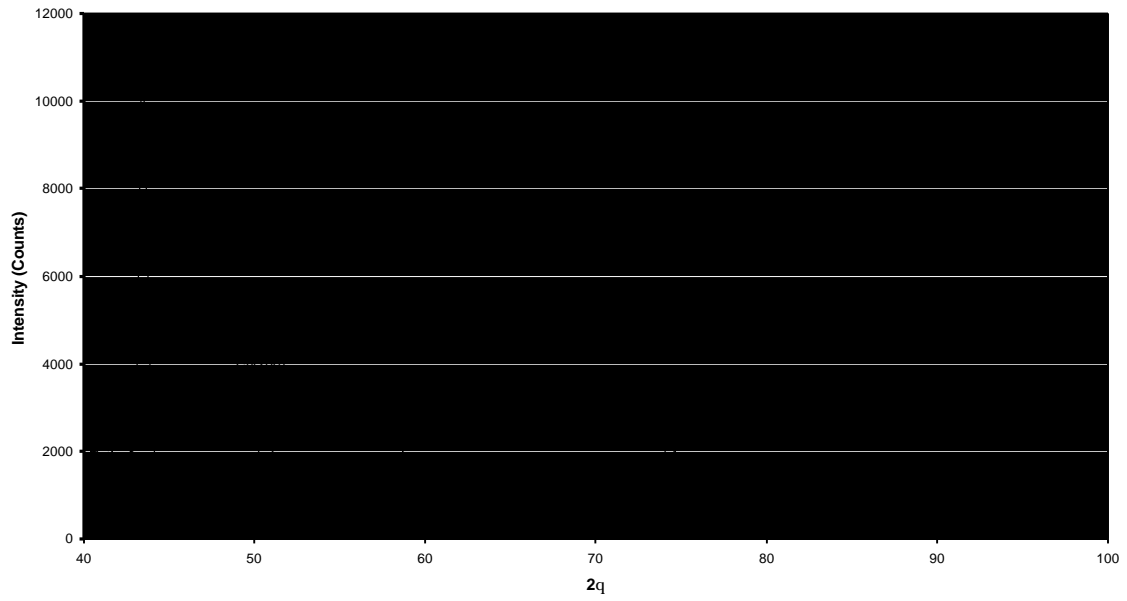


Figure 1(f)

(a)



(b)

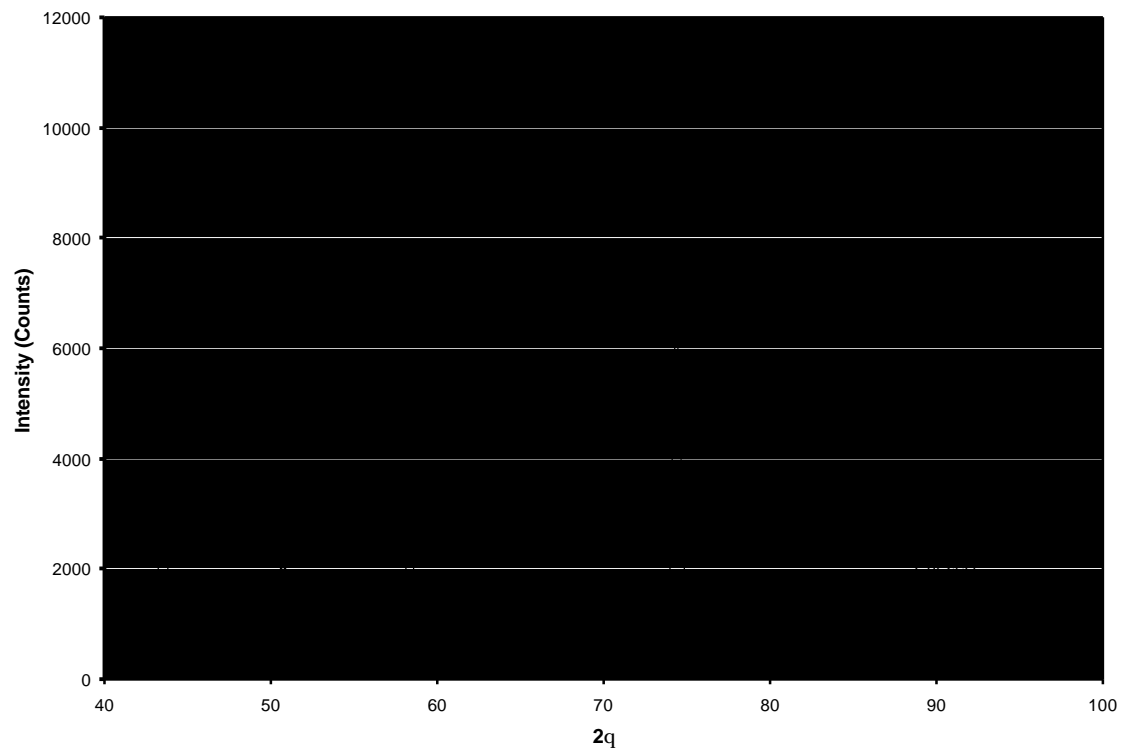


Figure 3 XRD patterns for (a) Cu film just deposited, (b) Cu bonded layer.

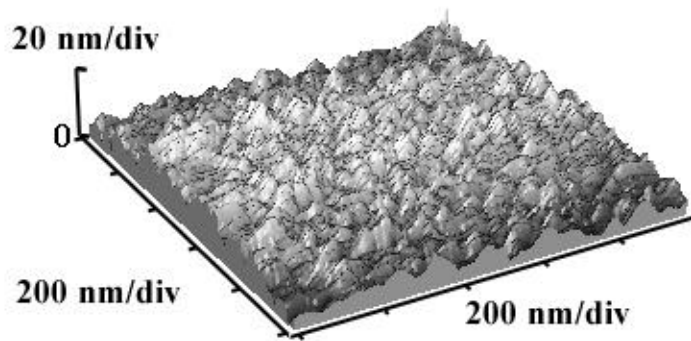


Figure 2 AFM image of the surface roughness of Cu film before bonding.

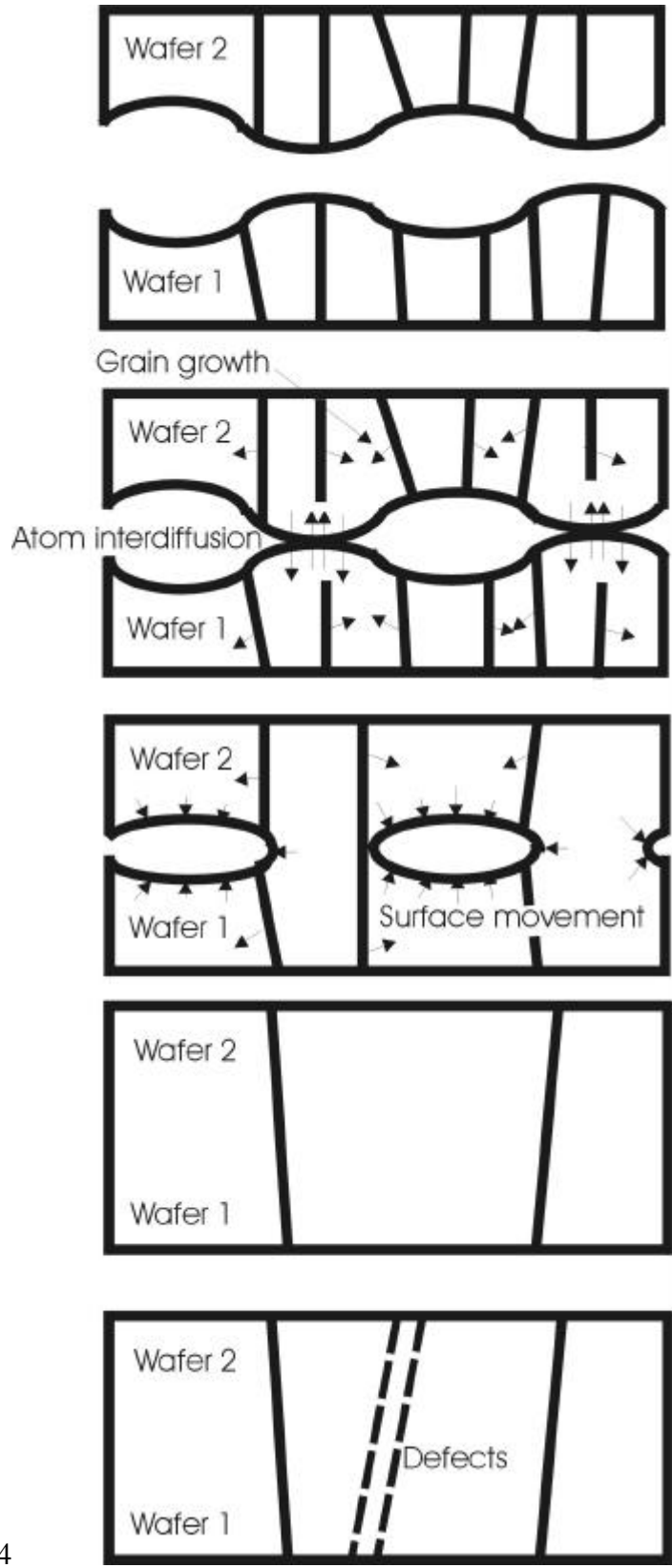


Figure 4

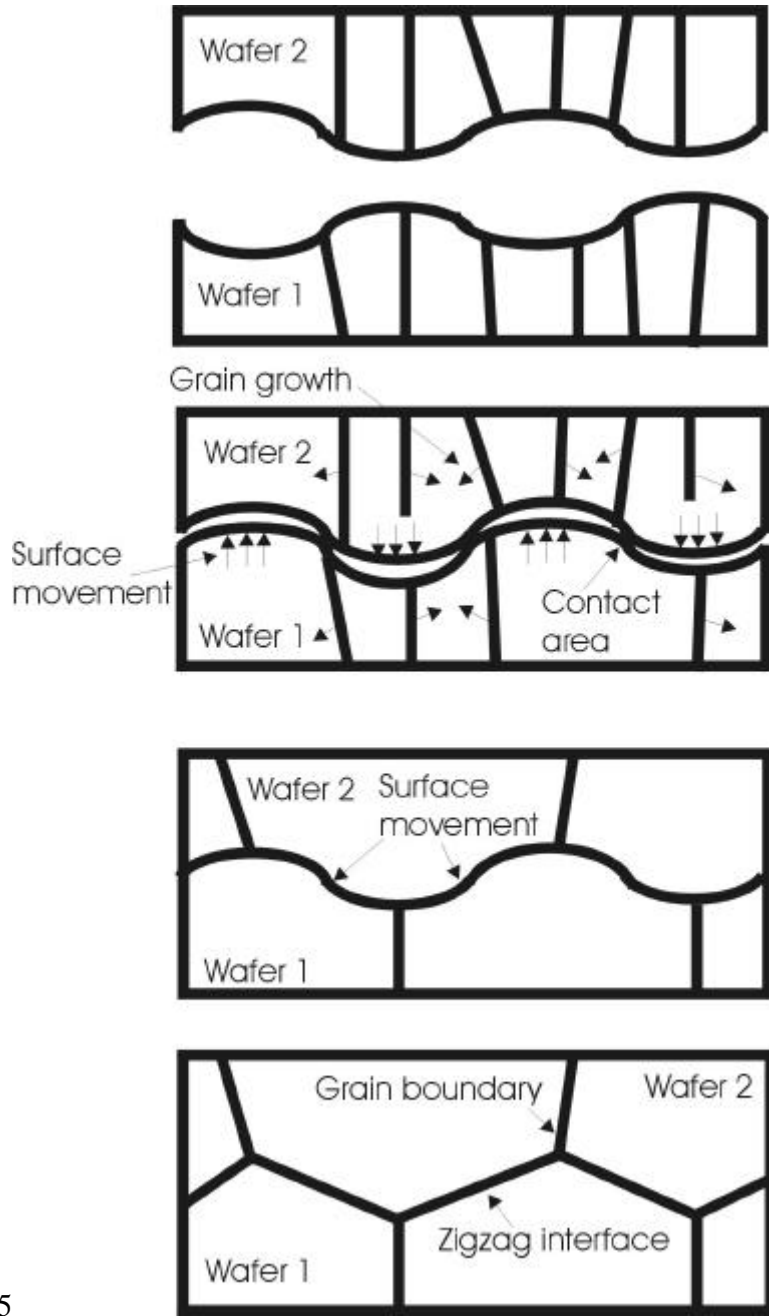


Figure 5

